Available online at www.sciencedirect.com
ScienceDirect
Acta Materialia 58 (2010) 6487–6494
Acta MATERIALIA
www.elsevier.com/locate/actamat

Material-dependent representative plastic strain for the prediction of indentation hardness

Nathan A. Branch, Ghatu Subhash *, Nagaraj K. Arakere, Michael A. Klecka

Department of Mechanical and Aerospace Engineering, University of Florida, Gainesville, FL 32611-6300, USA

Received 18 January 2010; received in revised form 4 August 2010; accepted 12 August 2010
Available online 7 September 2010

Abstract

The definition of representative plastic strain induced by a Vickers indent has received considerable attention in recent years. Previous reports have attempted to define a universal value that was independent of a material's plastic response. However, the work presented here will show that a material-dependent representative plastic strain is valid in the conversion of flow stress to indentation hardness. This representative plastic strain is the volume average plastic strain within the plastic zone of Vickers indentation. The increase in indentation hardness within the plastic zones of macro-indents was experimentally determined by micro-Vickers indentation and then compared with that predicted by finite element modeling, which utilizes the proposed representative plastic strain. It was further shown that the representative plastic strain defined here is independent of yield strength, elastic modulus and magnitude of prior plastic deformation for both linear and power law strain hardening materials.

Keywords: Representative plastic strain; Hardness; Plastic deformation; Finite element modeling

1. Introduction

Although surface indentation has frequently been used to estimate the elastic and plastic response of materials, the definition of the representative plastic strain induced by a Vickers indent has been a topic of considerable controversy and discussion [1]. Beginning with Tabor [2], many others [3–6] have shown that the constraint factor $C = H/\sigma_y$ is about 3 for most perfectly plastic engineering materials, where H is the Vickers indentation hardness and σ_y is the yield strength. This ratio also applies to strain hardening materials, where σ_y is replaced by a representative flow stress σ_r corresponding to a representative plastic strain ε_r. Tabor [2] proposed that a Vickers indent induces an additional representative plastic strain of 0.08 regardless of the initial plastic strain ε_p^i or indent depth d. This value for representative plastic strain is not the actual plastic deformation induced by the indent, but is a parameter that provides a statistical "best fit" to the measured increase in indentation hardness of plastically deformed, strain hardening materials. To predict the increase in hardness of a plastically deformed (pre-strained) material with respect to its virgin state, C is multiplied by the flow stress σ_r that corresponds to the sum total of the initial plastic strain ε_p^i plus the representative plastic strain induced by the Vickers indent. This predicted indentation hardness is represented by the equation:

$$\begin{cases} H = C\sigma_r|_{\varepsilon=\varepsilon_r}, & \varepsilon_p^i = 0 \\ H = C\sigma_r|_{\varepsilon=\varepsilon_r+\varepsilon_p^i}, & \varepsilon_p^i > 0 \end{cases} \tag{1}$$

where C is independent of initial plastic strain and indent depth due to the self-similarity of Vickers indenters [2].

Thus, the representative plastic strain induced by a Vickers indent describes the extent to which the representative flow stress over-predicts the yield strength of the indented material, as depicted in Fig. 1a. Similarly, when a material with an initial equivalent plastic strain ε_p^i is

* Corresponding author. Tel.: +1 352 392 7005; fax: +1 352 392 7303.
E-mail address: subhash@ufl.edu (G. Subhash).

1359-6454/$36.00 © 2010 Acta Materialia Inc. Published by Elsevier Ltd. All rights reserved.
doi:10.1016/j.actamat.2010.08.010

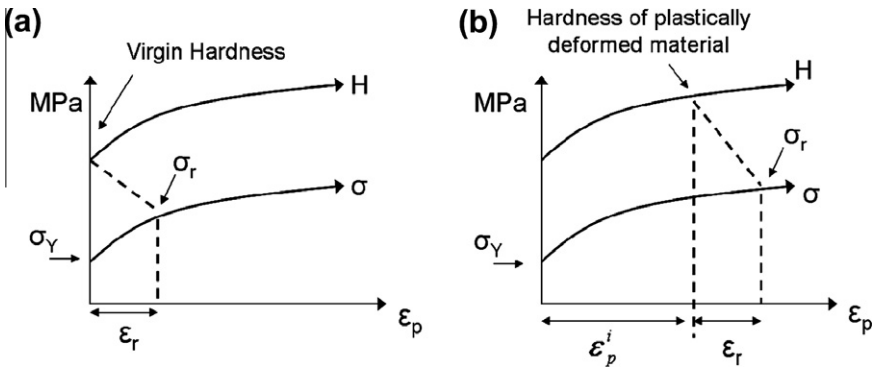

Fig. 1. Relationship between indentation hardness, flow stress and representative plastic strain for: (a) virgin ($\varepsilon_p^i = 0$) and (b) plastically deformed ($\varepsilon_p^i > 0$) materials.

subjected to a Vickers indent the same representative plastic strain is used to predict the increase in representative flow stress and indentation hardness, as depicted in Fig. 1b.

This process of estimating the increase in indentation hardness of a plastically deformed material when its flow curve is known a priori, is called a forward analysis. The opposite case where one wishes to predict a flow curve based on the indentation hardness of the deformed material is called a reverse analysis and is far more complicated to perform [7]. Many different forward and reverse analyses have been proposed since Tabor [2], and one of the most controversial topics in these methods is the manner in which the representative plastic strain was defined and calculated.

Representative plastic strain has been called by many different names: effective strain, average strain and characteristic strain [1,8]. Previous indentation methods that determined the plastic response of materials cannot agree on a single value for the representative plastic strain, but all concur that it estimates the increase in yield strength caused by plastic deformation of the indent [2,5,9].

Dao et al. [7] created dimensionless functions for both forward and reverse analyses for a range of material properties and determined that a universal representative plastic strain of 0.033 allowed the relationship between indentation loading curvature and reduced modulus to be independent of the strain hardening exponent (n) of the power law model $\sigma = K\varepsilon^n$, where K is the strength coefficient. Similar methods soon followed, most of which used different values for representative plastic strain. Bucaille et al. [10] extended their method to conical indenters with different included angles and showed that the representative plastic strain was dependent on indenter geometry. Ogasawara et al. [11] argued that the range of material properties used by Dao et al. [7] was too narrow and that their representative plastic strain was not associated with elastic or plastic deformation. They proposed a representative plastic strain value of 0.0115 that accounted for the biaxial nature of the plastic deformation due to Vickers indentation. In a subsequent paper, Ogasawara et al. [12] created new fitting 2functions derived from the elastic and plastic work of the indentation response for a single indenter while maintaining the same ε_r. Chollacoop and Ramamurty [9] showed how initial plastic deformation affected indentation loading curvature and that the method of Dao et al. [7] could be used to predict flow curves using two different indenters on strain hardening materials. Cao and Huber [13] determined that the representative plastic strain could be dependent on the ratio of loading curvature to reduced modulus and reported ε_r values in the range 0.023–0.095.

Other methods that did not use instrumented indentation proposed different values for representative plastic strain. Johnson [3] reported a representative plastic strain of 0.07 based on the boundary of the large hydrostatic stress "core" directly beneath the tip of a sharp indent. Chaudhri [1] suggested that the representative plastic strain should be the maximum plastic strain in the plastic zone of a Vickers indent and suggested values between 0.25 and 0.36. However, much higher maximum plastic strains have been observed to occur [7,10,14]. Using statistical fits in the relationship between normalized flow stress and hardness, Jayaraman et al. [8] determined a representative plastic strain of 0.07 and 0.225 for Berkovich and cube-corner indenters, respectively. The indentation hardness (converted to flow stress) from these two different indents at their respective representative plastic strains determined two points on the stress–strain curves of the indented materials. Tekkaya [15] proposed a value of $\varepsilon_r = 0.112$ based on their experiments that predicted the plastic strain magnitude and increase in indentation hardness associated with extrusion processes. Antunes et al. [16] also reported material-dependent representative plastic strain values ranging between 0.034 and 0.042.

The above proposed values for representative plastic strain are summarized in Table 1. Clearly, the values for representative plastic strain vary over a broad range. Most of the previous definitions of representative plastic strain were not based on a physical and measurable quantity. Rather, these parameters were calculated from curve fitting the indentation responses of a certain range of material properties. The "representative plastic strain" is really a misnomer in that it does not "represent" the actual plastic deformation within the plastic zone of a Vickers indent. Chaudhri [1] has dubbed Tabor's 0.08 strain an "undefined

Table 1
Summary of proposed values in the literature for representative plastic strain ε_r.

Reference	Value of ε_r
Tabor [2]	0.08
Dao et al. [7]	0.033
Ogasawara et al. [11]	0.0115
Cao and Huber [13]	0.023–0.095
Johnson [3]	0.07
Chaudhri [1]	0.25–0.36
Tekkaya [15]	0.112
Antunes et al. [16]	0.034–0.042

global value", whereas the 0.033 representative strain proposed by Dao et al. [7] has been called a "mathematical trick" having "no physical basis" [11,17]. Most of these methods attempted to find a universal value for representative plastic strain that works for all materials, however, the plastic strain induced by a Vickers indent (or other modes of plastic deformation) is highly dependent on the inherent resistance to plastic deformation of the indented material. Since this response is typically characterized by such parameters as the strain hardening exponent (n), a universal value for representative plastic strain is not expected to be valid for a wide range of materials which have different n values. Another drawback of the previous numerical methods is that they required the running of many finite element models along with the use of numerous dimensionless functions to characterize a given range of material responses which may not be all encompassing. In fact, research has shown that materials with different plastic responses can produce the same indentation loading curvature in single indenter methodologies [18], which rules out the uniqueness of such methods.

In the light of such difficulties there has been a strong desire to simplify indentation methodologies that are used to predict the plastic properties of materials and vice versa [19]. The method presented here defines the representative plastic strain as a calculable mathematical quantity of the plastic strain induced by a Vickers indent. This representative plastic strain is defined as the average volumetric equivalent plastic strain of the entire plastic zone, i.e.

$$\varepsilon_r = \frac{\sum \varepsilon_j V_j}{\sum V_j} \tag{2}$$

where ε_j is the equivalent plastic strain at the centroid of an elemental volume V_j within the plastic zone. Jayaraman et al. [8] suggested that this definition of average plastic strain is not a valid representative plastic strain because it is dependent on the strain hardening exponent and not universal to all materials. Because the plastic response to deformation (which is being characterized) is not the same for different strain hardening materials it is argued here that the representative plastic strain should not be a universal quantity and should thus be dependent on the material's capacity to strain harden. Accordingly, it cannot be assumed that a single representative plastic strain value will be valid for all types of materials. Jayaraman et al. [8] have shown that this average volumetric plastic strain is independent of elastic modulus and yield strength. It will be shown here that it is also independent of initial plastic strain for both linear and power law strain hardening materials.

In this analysis all plastic strains above 0.002 will be included in the determination of ε_r, which is consistent with the common definition of the 0.002 offset yield strength. Bucaille and Felder [14] used a similar definition of ε_r in their indentation simulations and scratch tests of perfectly plastic materials, but they limited their definition of ε_j to fall within the range $0.1\ \varepsilon^c_{eq} \leqslant \varepsilon_j \leqslant \varepsilon^c_{eq}$, where ε^c_{eq} is an arbitrarily chosen "critical plastic strain" in the range 0.1–2.5. They admitted that their definition of ε_j was highly dependent on the choice of critical plastic strain and consequently focused only on the ratio of ε_r when comparing scratch and indentation plastic zones. The representative plastic strain provided here in Eq. (2) is new and different in the sense that the entire plastic strain gradient within the plastic zone is accounted for in the calculation of representative plastic strain.

2. Forward analysis

A coordinated experimental and numerical approach was adopted to investigate the relationship between indentation hardness and a material's plastic response. First, macro-indents (at large loads in the range of several hundred kilograms) were performed on two virgin materials to create a large gradient in plastic strain within the indentation plastic zone. These specimens were sectioned slightly away from the indent center and gradually polished to the cross-section corresponding to the maximum plastic zone depth. The plastic strain magnitude beneath a macro-indent varies spatially over the plastic zone, with the highest plastic strains at the indenter tip, decreasing gradually with distance away from the tip. The increase in indentation hardness across this plastic strain gradient was determined by conducting micro-Vickers indents (at 200 g load) along the center line of the macro-indent plastic zone. In the next step a finite element model of the macro-indentation process used the constitutive response obtained from in-house compression tests to determine the resulting plastic strain gradient ε^i_p within the macro-indent plastic zone. Utilizing the definition of a material-dependent representative plastic strain (Eq. (2)) induced by the micro-Vickers indent, the increase in micro-Vickers hardness values was predicted via Eq. (1) and compared with those measured experimentally. Micro-Vickers indentations within this plastic zone were simulated to verify the representative plastic strain for pre-plastically deformed regions.

This study utilized both Vickers and Rockwell C macro-indenters to illustrate that the current procedure of predicting the increase in hardness within a plastic zone works irrespective of the method by which the plastic deformation is produced. Two commercially available materials, Pyrowear 675 Stainless Steel (P675 SS) with a power law strain

hardening response and 303 Stainless Steel (303 SS), which follows a linear strain hardening response, were used to validate a material-specific representative plastic strain on different strain hardening materials. P675 SS is typically case-hardened, but in the current analysis only the core (non-carburized) region with a homogeneous microstructure was investigated.

3. Experimental procedure

To induce a large plastic zone in the P675 SS specimen the Vickers indenter tip was fixed in a custom fabricated housing and mounted in a universal testing machine (MTS® Alliance™ RT/30). A load of 204 kg was used to create the desired macro-Vickers indent. The measured Vickers hardness was 433 HV. A standard Rockwell C macro-indent was produced on the 303 SS specimen using the standard 150 kg Rockwell C indent load, which resulted in a measured hardness of 26 HRC (275 HV). After indentation these macro-indented specimens were sectioned close to the indent and progressively polished to reveal the indent cross-section at the maximum indent depth. Standard metallographic polishing procedures using progressively smaller polishing media were utilized to minimize damage and residual stresses induced by grinding and polishing. To measure the increase in indentation hardness within these plastic zones micro-Vickers indents were conducted using a Wilson® Instruments (Tukon™ 2100 B) Vickers indenter at 200 g indent load and 15 s loading duration. As per ASTM standard ASTM E384, the micro-Vickers indents along the center line of the plastic zone were spaced 100 μm apart, as shown in Fig. 2, to prevent interaction with neighboring indents. Similar procedures for micro-indentation of the plastic zone beneath a macro-indent were also implemented by Chaudhri [1] and Srikant et al. [20].

The stress–strain curves obtained from in-house compression tests on P675 SS and 303 SS cylindrical specimens are shown in Fig. 3. Note that the P675 SS followed a power law model with strength coefficient $K = 1800$ MPa and strain hardening exponent $n = 0.064$ and the 303 stainless steel can be modeled as a linearly hardening material with a tangent modulus of 1183 MPa. The values for ε_r shown in Fig. 3 were calculated by importing these constitutive responses into the finite element models of the micro-Vickers indentation of these two materials.

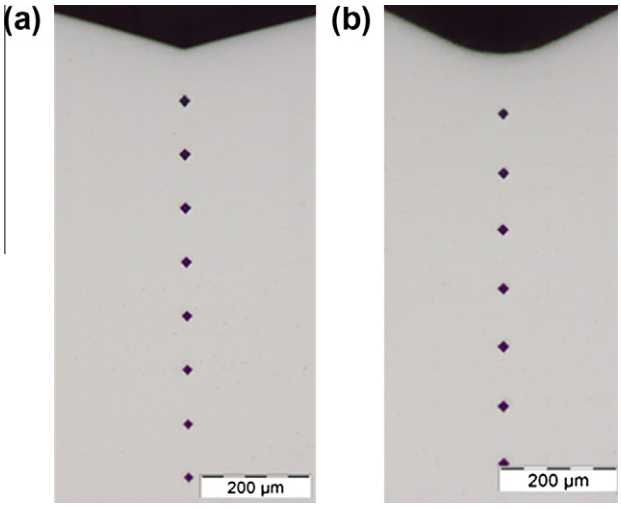

Fig. 2. Micro-Vickers indents within plastic zones of: (a) macro-Vickers indentation on P675 SS and (b) macro-Rockwell C indentation on 303 SS.

4. Finite element model

Recall that the purpose of the two macro-indents was to create two different plastic strain gradients on two materials. Therefore, two separate FE models were created to simulate the macro-Vickers indent on P675 SS (Fig. 4a) and Rockwell C macro-indent on 303 SS (Fig. 4b). Both indenters were displacement controlled to the same macro-indent depths as in the experiment and then retracted to their original positions. The indenters were given fixed rotational boundary conditions and only translated normal to the indented surface. A rigid indenter with an equivalent half cone angle of 70.3° produces the same projected indent area as a Vickers indent for any given indent depth and was used to simulate the macro-Vickers indent on P675 SS (Fig. 4a). For the Rockwell C indent a similar analysis was performed on the 303 SS model (Fig. 4b).

Five thousand four node bilinear quadrilateral axisymmetric elements made up the FE models, with the finest

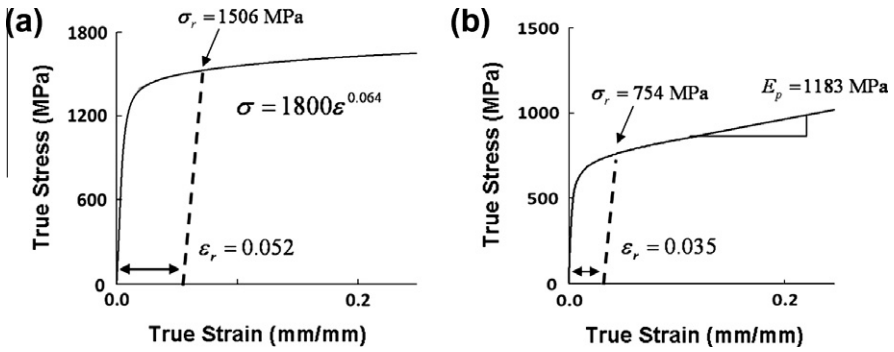

Fig. 3. Flow curves obtained by compression tests of: (a) P675 SS and (b) 303 SS.

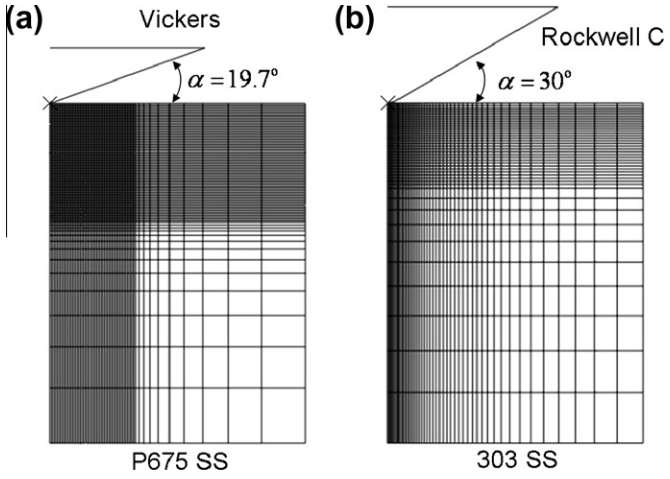

Fig. 4. Finite element meshes for: (a) macro-Vickers (P675 SS) and (b) macro-Rockwell C (303 SS) indents.

mesh in the region of the indented material. There were at least 20 elements in contact with the indenter during maximum indent depth, which provided sufficient resolution. The FE model was implemented in ABAQUS 6.7-1 and the plastic response of the material was governed by the von Mises (J2) yield criterion, associated flow rule, isotropic hardening and the constitutive responses obtained from the compression tests shown in Fig. 3 [21]. The micro-Vickers indents for both materials were also simulated in the plastically deformed and undeformed regions along the center line of the macro-indent plastic zones (Fig. 2) previously mentioned, using the same FE mesh and indent geometry as in Fig. 4a. These results will be used to verify the same representative plastic strain for both plastically deformed and virgin materials.

5. Results and discussion

The plastic strain contours below the macro-Vickers indent of P675 SS and Rockwell C macro-indent of 303 SS as calculated from the FE models are shown in Fig. 5a and b, respectively. Note that the plastic strain gradients were not the same due to differences in the plastic response of the two materials and indenter geometries. Because the indent depth was the same in the experiments and simulations, a direct comparison of the measured increase in micro-indentation hardness within these plastic zones could be made with those predicted by the FE model, but the representative plastic strain induced by the micro-Vickers indents must first be determined.

The representative plastic strain is the same for both micro and macro-Vickers indents, since the deformation by Vickers indentation is self-similar with respect to indent depth (excluding indentation size effects, which were not observed for these two materials at the chosen indent loads). As such, the depths of the plastic strain contours are non-dimensional with respect to indent depth in Fig. 6, in which the plastic strain contours around the micro-Vickers indents of both virgin P675 SS and 303 SS are shown. These plastic strain values, along with Eq. (2), were used to determine values for ε_r of 0.052 and 0.035 for P675 SS and 303 SS, respectively. These results compare well with the average plastic strain induced by Vickers indents calculated by Jayaraman et al. [8]. It will be shown later that this representative plastic strain was also independent of the initial plastic strain of the indented material. The corresponding representative flow stress σ_r (Fig. 3) and constraint factor $C = H/\sigma_r$ could be calculated as 2.8 and 3.5 for P675 SS and 303 SS, respectively. While the magnitudes of plastic strain contours in Fig. 6 are the same, the differences in spatial variation were due to the plastic responses of P675 SS and 303 SS (Fig. 3). P675 SS had a higher yield strength (1300 MPa) than 303 SS (600 MPa), but had a lower strain hardening rate ($n = 0.064$) than 303 SS ($E_p = 1183$ MPa). This caused the strain gradient to be slightly more severe below the Vickers indent tip in 303 SS (due to higher strain hardening), but more spread out (lower yield strength) when compared with P675 SS (Fig. 6).

The plastic strain gradient along the center line of each macro-indent plastic zone was used to predict the increase

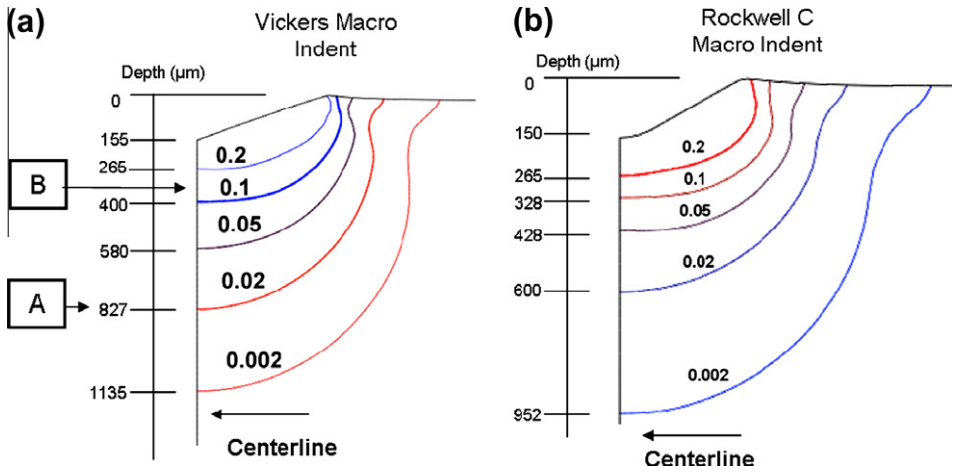

Fig. 5. Plastic strain contours beneath: (a) a macro-Vickers indent for P675 SS and (b) a macro-Rockwell C indent for 303 SS, respectively. Indent depths match those of the experimental macro-indents.

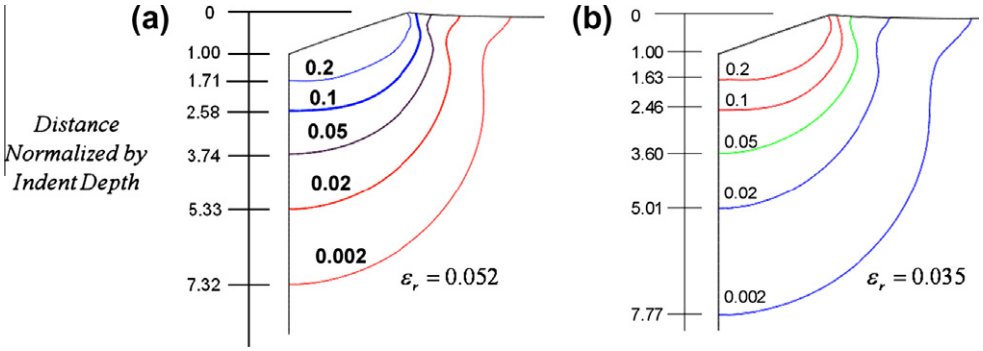

Fig. 6. Plastic strain contours below micro-Vickers indents of: (a) P675 SS and (b) 303 SS. Plastic strain contour depth is non-dimensional with respect to indent depth. These plastic strain gradients were used to determine the representative plastic strain ε_r (via Eq. (2)) induced by the micro-Vickers indents.

in micro-Vickers hardness using Eq. (1), where ε_p^i is the initial equivalent plastic strain along the center line of the plastic zone (Fig. 5) and ε_r is the material-specific representative plastic strain induced by the individual micro-Vickers indents (Fig. 6) at each micro-indent location. The predicted micro-indentation hardness values were compared with the experimentally measured hardness values along the center line of the plastic zone as shown in Fig. 7. There was good agreement between these values for both the Vickers and Rockwell C macro-indents, which validates the use of a material-dependent representative plastic strain.

The increase in indentation hardness as a function of plastic strain could be calculated using these results. Such information is useful in metal forming processes where local hardness measurements can be used to estimate the magnitude of equivalent plastic strain on a cold formed part [5]. The calculated Vickers hardness values as a function of plastic strain for P675 SS and 303 SS are shown in Fig. 8.

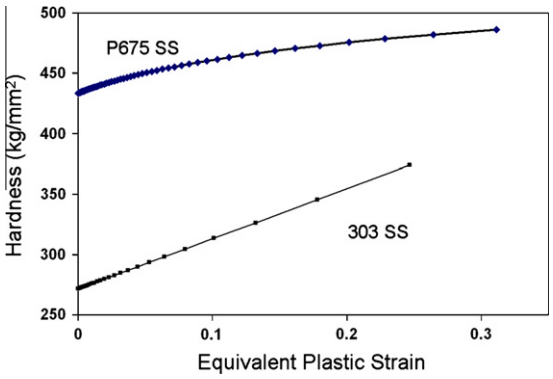

Fig. 8. Vickers indentation hardness as a function of equivalent plastic strain for P675 SS and 303 SS.

6. Representative plastic strain of an initially plastically deformed material

In the previous section the representative plastic strain ε_r was added to the initial local plastic strain ε_p^i to calculate the increase in micro-Vickers hardness (as per Eq. (1)) because the micro-indent plastically deformed and further strain hardened the initially plastically deformed region [2,5,9]. The representative plastic strain induced by the micro-Vickers indent was independent of the magnitude of the initial plastic strain of the indented material. To illustrate this point, the micro-Vickers indents at points along the center line of the plastic zone of the P675 SS macro-indent were simulated. At each location a uniform distribution of initial equivalent plastic strain magnitude over the small area of the micro-indent was assumed. The calculated equivalent plastic strain magnitudes at locations

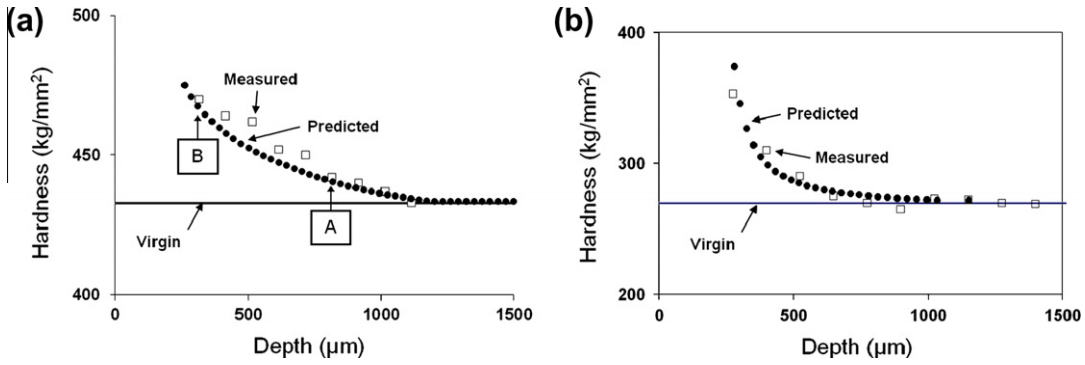

Fig. 7. Comparison between measured vs. predicted micro-Vickers hardness within the plastic zones of: (a) Vickers macro-indent for P675 SS and (b) Rockwell C macro-indent of 303 SS.

A and B were 0.02 and 0.146, as illustrated in Fig. 5a, and the experimentally measured Vickers hardness values were 442 and 470 HV, respectively (Fig. 7a). The same FE mesh of Vickers indentation from Fig. 4a was used again for the simulations of the micro-Vickers indents of the pre-strained points (A and B), except radial plastic strain magnitudes of 0.01 and 0.073 were now applied to plastically strain harden the material to the equivalent plastic strain states of 0.02 and 0.146, respectively, prior to indentation (Fig. 9), as predicted by Cauchy's strain displacement equations. The elastic recovery was also simulated in order to keep residual stresses close to zero in these models, to avoid any influences due to residual stresses on the calculation of the additional plastic strain due to the Vickers indent.

The modified Eq. (2) is then written as:

$$\varepsilon_r = \frac{\sum(\varepsilon_j - \varepsilon_p^i)V_j}{\sum V_j} \tag{3}$$

where ε_p^i is the initial equivalent plastic strain magnitude (0.02 or 0.146) of the indented material, which must be subtracted from the total equivalent plastic strain at every point within the new plastic zone to determine the contribution of the additional plastic strain induced by the Vickers micro-indent at locations A and B. The representative plastic strain induced by the Vickers micro-indent was calculated and found to be the same as that of the virgin material, i.e. $\varepsilon_r = 0.052$ for both points A and B of the pre-deformed P675 SS material. Fig. 10 shows the additional plastic zone induced by the Vickers micro-indent at point B with an initial pre-plastic strain of 0.146. Note that the plastic strain gradient is similar to that of the virgin material (Fig. 6a), in the sense that the plastic strain contours shown have an increased plastic strain magnitude of 0.146 at relatively the same locations within its plastic zone. However, the plastic zone in Fig. 10 is shallower with respect to indent depth due to the strain hardening and increased yield strength of point B prior to indentation. Interestingly, the representative plastic strain (average additional plastic strain) remains the same as calculated by Eq. (3).

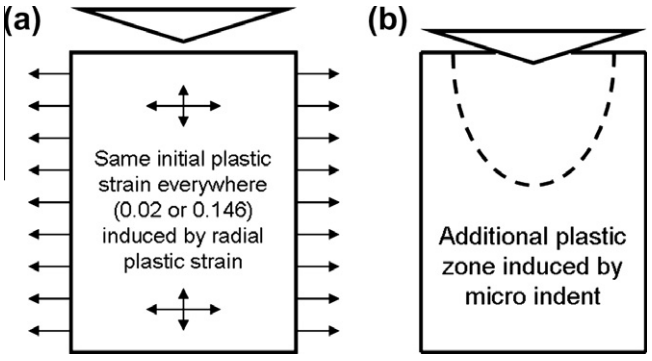

Fig. 9. Schematic of the micro-Vickers indent of a pre-strained material: (a) region with the same initial equivalent plastic strain throughout the material prior to indentation and (b) illustration of additional plastic strain induced by the micro-indent.

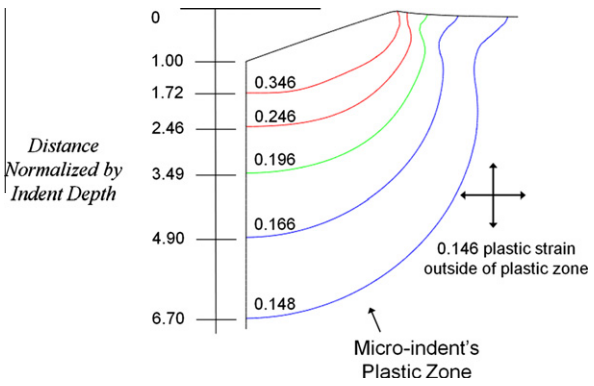

Fig. 10. Plastic strain contours of Vickers micro-indent on pre-plastically strained P675 SS at point B in Figs. 5 and 7. Depth is non-dimensional with respect to indent depth.

This exercise clearly demonstrates that the representative plastic strain induced by a Vickers micro-indent is independent of the initial plastic strain within the indented material. Even though this method has been shown to work for plastic gradients induced by indents, it can also predict the increased indentation hardness of any plastically deformed region caused by compression, tension, torsion, bending or complex cold forming processes, provided the loading is not cyclical in nature (i.e. monotonic loading). Vickers and Rockwell C macro-indentations were chosen in these experiments because they are relatively simple and inexpensive to produce and can create controlled and convenient plastic strain gradients with plastic strains as high as 0.4. Such large plastic strains may otherwise be unobtainable in tension or compression tests or other modes of deformation. The large hydrostatic stresses and confinement associated with indentation prevent premature failure and make these high plastic strains possible. Moreover, these plastic zones are relatively small in size, which allows multiple tests on a single specimen. Previous indentation methods did not examine the plastic zone of pre-plastically deformed materials in this detail, nor has anyone verified the assumption that the representative plastic strain used here is not a function of initial plastic strain using finite element models of experimental Vickers indentation.

7. Conclusions

Unlike previous methods, which attempted to find a universal value of representative plastic strain for all types of materials, the material-dependent average plastic strain of a plastic zone caused by a Vickers indent has been shown to be a valid representative plastic strain in the prediction of Vickers indentation hardness. The method presented here accurately predicts the increase in indentation hardness within the plastic zones of both Vickers and Rockwell C indents for both linear and power law strain hardening materials. The predicted indentation hardness compared well with experimentally measured micro-Vickers indent mapping for the plastic zones of P675 SS and 303 SS. The simulations of the micro-indents along the center line

of the plastic zone of the P675 SS material proved that the representative plastic strain used here is independent of the amount of prior plastic deformation of the indented material.

Acknowledgements

This work was partially supported by National Science Foundation Award CMMI-0927849 under program officer Dr. Clark V. Cooper. The authors express their gratitude to Dr. Nelson Forster, Vaughn Svendsen and Dr. Lewis Rosado of AFRL for their contributions to this project. Thanks are also due to Dr. William Hannon, Dr. Liz Cooke and Bob Wolfe of Timken Co. for their continued support of this work. Sincere thanks go to Bill Ogden, Herb Chin and David Haluck of Pratt & Whitney for their interest and support of this research.

References

[1] Chaudhri MM. Acta Mater 1998;46(9):3047.
[2] Tabor D. Rev Phys Technol 1970;1:145.
[3] Johnson KL. Contact mechanics. Cambridge: Cambridge University Press; 1985.
[4] Gao XL, Jing XN, Subhash G. Int J Solids Struct 2006;43:2193.
[5] Sonmez F, Demir AJ. Mater Process Technol 2007;186:163.
[6] Pavlina EJ, Van Tyne CJJ. Mater Eng Perform 2008;17(6):888.
[7] Dao M, Chollacoop N, Van Vliet KJ, Venkatesh TA, Suresh S. Acta Mater 2001;49:3899.
[8] Jayaraman S, Hahn GT, Oliver WC, Rubin CA, Bastias PC. IJSS 1998;35(5/6):365.
[9] Chollacoop N, Ramamurty U. Scr Mater 2005;53:247.
[10] Bucaille JL, Stauss S, Felder E, Michler J. Acta Mater 2003;51:1663.
[11] Ogasawara N, Chiba N, Chen XJ. Mater Res 2005;20(8):2225.
[12] Ogasawara N, Chiba N, Chen X. Scr Mater 2006;54:65.
[13] Cao T, Huber N. J Mater Res 2006;21(7):1810.
[14] Bucaille JL, Felder E. Philos Mag A 2002;82(10):2003.
[15] Tekkaya AE. CIRP Ann Manuf Technol 2000;1(1):205.
[16] Antunes JM, Fernandes JV, Menezes LF, Chaparro BM. Acta Mater 2007;55:69.
[17] Ogasawara N, Chiba N, Zhao M, Chen XJ. Solid Mech Mater Eng 2007;1(7):1618.
[18] Chollacoop N, Dao M, Suresh S. Acta Mater 2003;51:3713.
[19] Baxevani EA, Giannakopoulos AE. Exp Mech 2009;49:371.
[20] Srikant G, Chollacoop N, Ramamurty U. Acta Mater 2006;54:5171.
[21] Dassault Systèmes. ABAQUS theory manual V6.7-1. Providence, RI: DS Simulia Corp.; 2007.